

The Weakly Coupled Channels Contribution Effects in Neutron Induced Complex Particles Emission in ^{98}Mo Nuclei

Mahdi Hadi Jasim

University of Baghdad, College of Science, Department of Physics

Abstract: The non-equidistant space model (non-ESM) for two-component state densities has been modified to include different correction parameters. The calculated results have been used with neutron induced reaction with ^{56}Fe target nuclei. The comparisons with other theoretical and experimental results show a very good agreement at excitation energy less than 15 MeV. The modified state density has been applied to calculate the cross-sections of emitting a complex particles in $^{98}\text{Mo}(n,n+p)^{97}\text{Nb}^m$ and $^{98}\text{Mo}(n,^4\text{He})^{96}\text{Zr}$ reactions for different incident neutron energies. Furthermore, the results are compared with the available experimental results of EXFOR. It was found the weaker probability of emitting complex particles comes from weaker primary pre-equilibrium emission due to high binding energies of complex particles. Different stages of probabilities for neutron induced complex particles emissions have been studied to evaluate the depletion factor DF that weakly contributed from the direct or PE processes in (neutron + ^{98}Mo) reaction by consume the flux in complex emission particles, $(n+p)$ and (^4He).

Keywords: Depletion factor, Pre-Equilibrium fraction, $^{98}\text{Mo}(n,n+p)^{97}\text{Nb}^m$ and $^{98}\text{Mo}(n,^4\text{He})^{96}\text{Zr}$ reactions

1. Introduction

Griffin proposed a semi-classical approach to explain and predicted the probability of the pre-equilibrium (PE) region toward the tracking and understanding the scattering process at equilibrium stage [1]. This approach is called exciton model (ExM), which is assumed the incident projectile on a certain target nuclei gradually induced more excited states in the frame of the compound system. These excited states are characterized by excitation energy and the exciton number [$n=p$ (particle)+ h (hole)] below the Fermi energy (ϵ_F). Base on experimental results of light nuclei-target nuclei at different excitation energies, this model has been reformulated and included system properties and features [2-5]. Furthermore, Griffin's model is integrated with quantum mechanic's approaches to describe the state density of the possible PE channels of reactions [6]. This development of ExM gathered the idea of equidistant space model (ESM) and non-equidistant space model (NESM) which gave promising and satisfactory results [7-9]. The addition of the Feshbach, Kerman, Koonin theory (FKK- theory) with ExM gave more improvements to the probabilities' predictions of the reaction channels. The idea of multistep direct (MSD) and multistep compound (MSC) stages of this model is succeeded in justification the appearance of particles involved in the reaction at short time and high energy. In MSD, most of the particles involved in the reactions are unbound with at least one particle is bound, and a significant forward peak may be achieved. While in MSC stage, all particles are bound and the emission is rather slow with continuous distribution or symmetric about 90° .

The ExM has been developed with different physical corrections, such as, Pauli's correction [10], implication of the angular momentum dependence [11], developed a method to calculate by master equation [12], back shift [13], surface correction [14], bound state correction and finite depth [15], the extension to the two-component formalism [16], the distinction of neutron and proton through the

reaction chained the implication of the extension to gamma-ray emission [17], pairing correction [18] and isospin distribution and parity corrections [18-20].

2. Theory

The depletion factor, DF, is applied to the weakly coupled channels that deplete the flux, such as contributions from the direct or PE processes. For the deformed nuclides, the effect of direct transitions to discrete levels is included directly in the coupled-channels scheme and the $\sigma_{\text{dis+dir}}$ is omitted in this equation. Then, the DF can formulate as:

$$DF = 1 - \left(\frac{\sigma_{\text{dis+dir}}}{\sigma_{\text{rxn}}} + \frac{\sigma_{\text{PE}}}{\sigma_{\text{rxn}}} \right) \quad (1)$$

where the $\sigma_{\text{dis+dir}}$ is the total discrete and direct reaction cross-section, σ_{PE} is the PE cross-section and σ_{rxn} is the reaction cross-section.

In order to calculate equation (1), the following formulae are considered.

a) The PE cross-section

The quantum mechanical theories have been developed to describe pre-equilibrium processes. The most used theory is that of FKK [19]. The theory partitions the reaction process into two types of scattering: multistep compound (important at the lowest incident energies), and multistep direct (important at higher incident energies). The above theory of reactions will be applied to the spectrum calculations. The PE cross-section is formulated in terms of The MSD and MSC differential cross-section can be formulated as [21]:

$$\left(\frac{d\sigma}{d\epsilon} \right)_{\text{MSD}} = \sum_{i=1}^3 \left(\frac{d\sigma}{d\epsilon} \right)_i \quad \text{and} \quad \left(\frac{d\sigma}{d\epsilon} \right)_{\text{MSC}} = \sum_{i=1}^2 \left(\frac{d\sigma}{d\epsilon} \right)_i \quad (2)$$

Where $i=1,2,3$ for primary and secondary PE, and knockout or direct differential cross-sections, respectively.

When the cross-sections in eq.(2) are combined in the forward peak for the energy channel particle b (ϵ_b) the fraction yields;

$$f_{PE}(\epsilon_b) = \frac{\left(\frac{d\sigma}{d\epsilon}\right)_{MSD}}{\left(\frac{d\sigma}{d\epsilon}\right)_{MSD} + \left(\frac{d\sigma}{d\epsilon}\right)_{MSC}} \quad (3)$$

$$\frac{d\sigma_b^{PE}}{dE_b} = \sigma^{CF}(\epsilon_a) \sum_{p_\pi = p_\pi^0}^{p_\pi^{max}} \sum_{p_\nu = p_\nu^0}^{p_\nu^{max}} W_b(p_\pi, h_\pi, p_\nu, h_\nu, E^{tot}, E_b, T) \times \tau(p_\pi, h_\pi, p_\nu, h_\nu) \times P(p_\pi, h_\pi, p_\nu, h_\nu) \quad (4)$$

where the factor P represents the part of the PE population that has survived emission, the compound formation cross section σ^{CF} , $\sigma^{CF}(\epsilon_a) = \sigma_{rxn} - \sigma_{dire}$, σ_{rxn} is the reaction cross-section can be obtained from the optical model using the Neutron Spherical Optical-Statistical Model (ABAREX-code system) [15].

$$W_b(p_\pi, h_\pi, p_\nu, h_\nu, E^{tot}, E_b, T) = \frac{2\epsilon_b + 1}{\pi^2} \mu_b E_b \sigma_{b,inv}(E_b) \times \sum_T |C_b(T, T_B)|^2 \frac{\Omega(p_\pi - Z_b, h_\pi, p_\nu - N_b, h_\nu, U, T_B)}{\Omega(p_\pi, h_\pi, p_\nu, h_\nu, E, T)} \quad (5)$$

where $\sigma_{b,inv}(E_b)$ is the inverse reaction cross section, Z_b (N_b) is the charge (neutron) number of the emission particle b, U is residual excitation energy $U = E - \epsilon - B_b$, E is the system excitation energy, ϵ is the single particle energy, B_b is the binding energy of emitted particles., $(C_b(T, T_B))$ is the isospin coupling Clebsch-Gorden coefficient for emitted particle b, $\Omega(p_\pi - Z_b, h_\pi, p_\nu - N_b, h_\nu, U, T_B)$ is the NESM two component total state density for the particle b with atomic number and number of neutron reduction $(p_\pi - Z_b, p_\nu - N_b)$, respectively and corrected for the finite

The primary PE differential cross section, for the emission of a cluster particle b with emission energy E_b and can then be expressed in terms of lifetimes τ for various classes of stages, with the composite nucleus formation cross section σ^{CF} and an emission rate ζ_b in two-component, can be defined as :

The emission rate, W_b , (Cline and Blann [16], from a state in the isospin mixed case that has the form of the particle b emission rate at the equilibrium stage with relative reduced mass μ_b , spin s_b , isospin quantum number T and the final state isospin T_B is:

well depth, isospin, shell effects, Pauli effect, charge effect, pairing, surface, angular and linear momentum distributions corrections are considered in this work and $\Omega(p_\pi, h_\pi, p_\nu, h_\nu, E, T)$ is the two component total state density for the final state, and the ratio of Ω is called branching ratio. The NESM total state density is developed in the present work and became as:

$$\Omega(p, h, E) = \frac{g_o^n}{2^n \pi^{n/2} p! h!} \equiv \frac{E^{N-1}}{F^{N-n}(N-1)!} \quad (6)$$

where the mathematical multiplication operator \equiv , $\equiv \equiv \sum_{\substack{\alpha_1, \alpha_2, \dots, \alpha_n \\ \beta_1, \beta_2, \dots, \beta_n=0}}^{\infty} \prod_{j=1}^p C_{\alpha_j}^p \prod_{l=1}^h C_{\beta_l}^h$

where $C_{\alpha_j}^p$ and $C_{\beta_l}^h$ are the coefficients for the expansion the p-h single level density,

$$g_p(\bar{\epsilon}_p) = g \sum_{n=0}^{\infty} \binom{1/2}{n} \left(\frac{\bar{\epsilon}_p}{F}\right)^n, \quad g_h(\bar{\epsilon}_h) = g \sum_{n=0}^{\infty} (-1)^n \binom{1/2}{n} \left(\frac{\bar{\epsilon}_h}{F}\right)^n$$

Over the most probable of (p,h) configurations and in terms of fermi energy, F, and single level density, g_0 , at F. This formula has been established depending on the different modifications and ideas, [22-25].

$$\sigma_b(\epsilon) = \begin{cases} 0 & \text{for } E_L \leq E_{bmin} \\ \kappa E_L^2 + \alpha E_L + \beta & \text{for } E_{bmin} \leq E_L < B_{coul,a} \\ \lambda E_L + \mu + \frac{\delta}{E_L} & \text{for } B_{coul,a} \leq E_L \leq E_{btest} \\ \max\left(\lambda E_L + \mu + \frac{\delta}{E_L}, \sigma_g\right) & \text{for } E_{btest} < E_L \end{cases} \quad (7)$$

The variables α and β are given by:

$$\beta = \kappa B_{coul,a}^2 + \mu + \frac{2\delta}{B_{coul,a}} \quad \text{and} \quad E_{bmin} = \begin{cases} (-\alpha + \sqrt{\alpha^2 - 4\kappa\beta})/2\kappa, & \alpha^2 - 4\kappa\beta > 0 \\ -\alpha/2\kappa, & \alpha^2 - 4\kappa\beta \leq 0 \end{cases}$$

The parameters $\kappa, \lambda, \mu, \nu, B_{coul,a}$ and E_{btest} are listed in table (1). The quantities $\kappa_0, \kappa_1, \kappa_2, \mu_0, \mu_1, \nu_0, \nu_1$, and ν_2 can be find in [21].

The geometrical cross section is given by [21]:

$$\sigma_g = \pi [R_{tar} + r_a]^2 \quad (8)$$

where, R_{tar} and r_a are the target and projectile radius, respectively [26,27,28].

Table 1: The parameters used in calculating the reaction cross section [21]

variable	Neutron	Proton
$B_{coul,a}$	0.5 MeV	$1.44Z_a Z_{tar} / [1.5A_{tar}^{1/3} + R_a]$; $R_{tar} = r_0 A_{tar}^{1/3}$
E_{btest}	32 MeV	$\sqrt{v/\lambda + 7}$ (proton) $1.2\sqrt{v/\lambda}$ (d, T, α)
κ	κ_0	$\kappa_0 + \kappa_1/B_{coul,a} + \kappa_2/B_{coul,a}^2$
λ	$\lambda_0 A_{tar}^{-1/3} + \lambda_1$	$\lambda_0 + A_{tar} + \lambda_1$
μ	$\mu_0 A_{tar}^{1/3} + \mu_1 A_{tar}^{2/3}$	$\mu_0 A_{tar}^{\mu_1}$
ν	$\nu_0 A_{tar}^{4/3} + \nu_1 A_{tar}^{2/3} + \nu_2$	$A_{tar}^{\mu_1} [\nu_0 + \nu_1 B_{coul,a} + \nu_2 B_{coul,a}^2]$

c) Knockout or Direct reaction stage

This stage includes two possible processes (i) the nucleon transfer (NT) mechanism and (ii) the Knockout process (KO). The first one includes direct pickup or stripping up to three nucleons, if the projectile (a) and the emitted particle

$$\left[\frac{d\sigma_{a,b}(\varepsilon)}{d\varepsilon} \right]_{NT} = \frac{2s_b + 1}{2s_a + 1} \frac{A_b}{A_a} \varepsilon \sigma_b(\varepsilon) K_{\alpha,p} \left(\frac{A_a}{E_a + V_a} \right)^{2n} \left(\frac{C_a}{A_B} \right)^n N_a \sum_{p_\pi} \left(\frac{2Z_A}{A_A} \right)^{2(Z_a+2)h_\pi+2p_\nu} \omega_{NT}(n,U) \quad (9)$$

where $\sigma_b(\varepsilon)$ is the inverse cross section, $K_{\alpha,p}$ is the enhancement factor for (α , N) and (N, α) reactions, E_a is incident energy in the laboratory system, V_a is the average potential drop seen by projectile between infinity and Fermi's level, C_a and N_a are the normalization constants can be

$$\left[\frac{d\sigma}{d\varepsilon} \right]_{KO} = \frac{\sigma_a(\varepsilon_a)}{14} (2s_b + 1) A_b \varepsilon \sigma_b(\varepsilon) \frac{\mathcal{P}_b g_a g_b [U - A_{KO}(p_a, h_b)]}{\sum_{c=a,b} (2s_c + 1) A_c (\sigma_c)(\varepsilon_m + 2B_{coul,c})} \times \frac{1}{(\varepsilon_m - B_{coul,c})^2 g_a g_b / 6 g_c} \quad (10)$$

where \mathcal{P}_b is the probability of exciting a b-type particle-hole pair, $\mathcal{P}_n \cong \frac{N_A}{A_A}$, $\mathcal{P}_p \cong \frac{Z_A}{A_A}$, $\mathcal{P}_\alpha \cong \frac{\phi Z_A}{2A_A}$, where ϕ is the possible fraction of the α -clusters that will exist at any given time, ε_m is the maximum emission energy, $B_{coul,c}$ is the coulomb barrier of type c, (σ_c) is the inverse cross-section, where a particle c is emitted, A_{KO} is the energy independent Pauli correction function, $A_{KO}(p_a, h_b) = \frac{1}{2g_a} + \frac{1}{2g_b}$, g_a and g_b are the single level density for a,b- type particles.

d) The equilibrium stage

In the equilibrium stage a Weisskopf-Ewing evaporation formula with isospin mixed particle emission rates is considered in this stage [31]:

$$W_b(E, \varepsilon) = \frac{2s_b + 1}{\pi^2 h^3} \mu_b \varepsilon \sigma_b(\varepsilon_b) \frac{\Omega(U)}{\Omega(E)} \quad (11)$$

Where $\Omega(U)$ and $\Omega(E)$ are the state densities for the residual nucleus and the emitting nucleus, respectively. In Fermi gas model the equilibrium state density has the form [32]:

$$\Omega_{FGM}(E) \propto a_0^{-1/4} E_{eff}^{-5/4} \exp(2\sqrt{a_0 E_{eff}}) \quad (12)$$

where a_0 is the level density parameter, $a_0 = \pi^2 g_0 / 6 = \pi^2 (g_{\pi 0} + g_{\nu 0}) / 6$, E_{eff} is the effective excitation energy with shell correction [33]. All the parameters are the same as the ones used in pre-equilibrium reaction.

(b) have different mass numbers; inelastic scattering (IN) for the light projectiles and charge exchanges reactions [26]. For the reaction A(a,b)B the general NT formula for energy spectrum:

determined by references [29] While in the second process, knock out process, the projectile will excite a proton, neutron or clusters in the target and resulting particles in the composite nucleus the can be emitted. The energy spectrum for this process has the form [30]:

3. Results and Discussions

In the present work the two-component state density, using the non-ESM exciton model, eq.(6), for neutron induced reactions with ^{56}Fe target nuclei has been compared with other theoretical and experimental results, see fig.1. The comparisons look at very good agreement at excitation energy less than 15 MeV. After adding all the corrections to the state density equation and compare the results with other practical data and theoretical results, eq.(4), it was found that the most important corrections need to be added to the state density and later enhanced the spectrum are: The Pauli, pairing, surface, back shift, isospin, and finite depth corrections.

After added the corrections to the state density equation, the calculated energy spectrums were also corrected, eqs.(5,7,8,9,10,11) and table (1). As shown in fig.2, the results are compared with a large variety of experimental data and theoretical data through the reference [40]. As shown in fig.2, in case of different incident neutron energies the probabilities of emitting the complex particles in (n,n+p) and (n, ^4He) reactions have low values due to facts that the probabilities of primary PE emission for (n+p) and (^4He) channels are weaker than that for nucleon channel; this means the secondary emission of complex particles is also weak. The weakness here is due to higher binding energy of complex particles on the exit channel.

In fig.3, the inter-comparison has been made from the data calculated in the present work for $^{98}\text{Mo}(n,n)^{98}\text{Mo}$ energy

spectrum, with the experimental measured data from EXFOR [40].

The DF for weakly coupled channel's energy spectrum that depletes the flux, eq.(1), which contributed from the direct or pre-equilibrium processes and PE factor,eq.(3), is shown in fig.4, where the spectrum of the depleted flux decreased as the energy shares the nucleons in the discrete excited states is increased. From this figure, one can indicate the dominant weakly depleted flux in incident neutron energy below 20 MeV. Furthermore, as shown in fig.5 the distribution of σ_{rxn} , σ_{dir} , σ_{PE} , σ_{disc} and $\sigma_{compound}$ cross-sections as a function of incident neutrons. It shows the weakly depleted probability increase and the PE probability decrease as the neutron energy less than 20MeV.

4. Conclusion

Different corrections have been implemented in predicting the state density, for the configuration of emitting complex particles, to compute and evaluate the cross-section in neutron interacted with ^{98}Mo target nuclei. From the behavior of the emitting ^4He and $(n+p)$ spectrums, it was concluded the weaker probability of these particles came from the weaker primary PE emission due to high binding energy of complex particles. Also, due to consume the flux in complex emission particles, $(n+p)$ and (^4He) , the depletion factors DF, that weakly contributed from the direct or PE processes in $(\text{neutron} + ^{98}\text{Mo})$ reaction, is increased at incident neutron energy less than 20 MeV, where the PE fractions in forward direction are decreased, and conversely at neutron energy greater than 20 MeV.

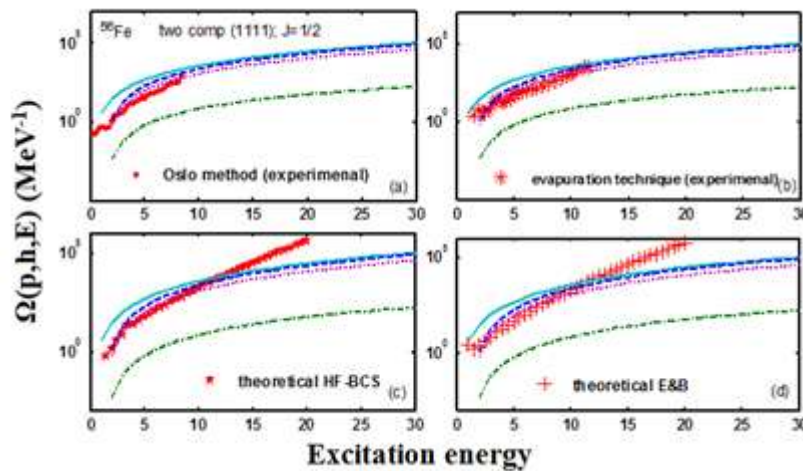


Figure 1: The two component state density as a function of excitation energy using eq.(6)

Solid curves: $\Omega(p,h,E)$ without any correction; dashed curves: with energy single particle level density (EDSPLD), pairing and finite depth corrections; dotted curves: represent the state density with EDSPLD, pairing and finite depth and parity corrections only; dashed dotted curves: with

EDSPLD, pairing, finite depth and spin distribution corrections. These results are compared with experimental data in (a) [34,35] and (b)[36,39], also with other theoretical results (c) [37] and (d)[38].

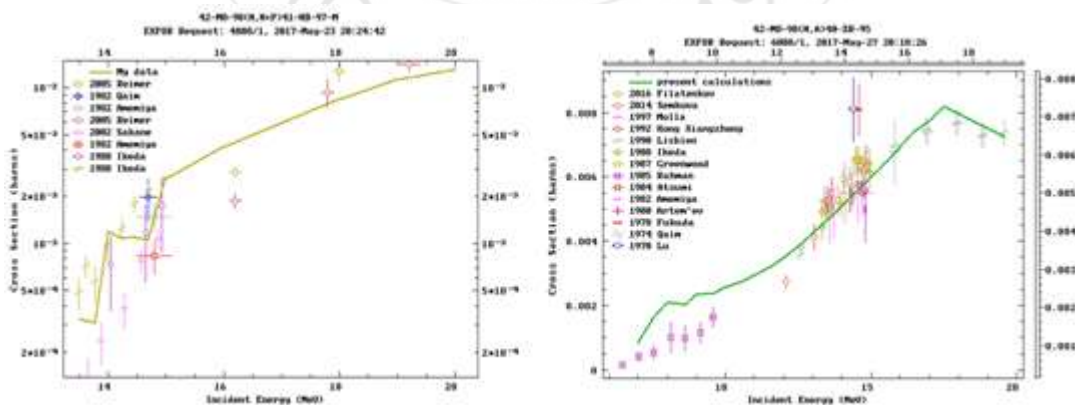


Figure 2: The $^{98}\text{Mo} (n, n + p) ^{97}\text{Nb}^m$ and $^{98}\text{Mo} (n, ^4\text{He}) ^{95}\text{Zr}$ cross-sections at different incident neutrons compared with data for EXFOR [40].

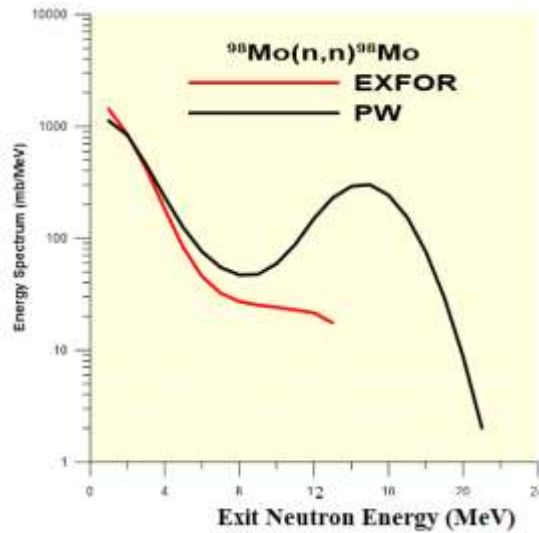


Figure 3: The $^{98}\text{Mo}(n,n)^{98}\text{Mo}$ energy spectrum compared with data for EXFOR[40]

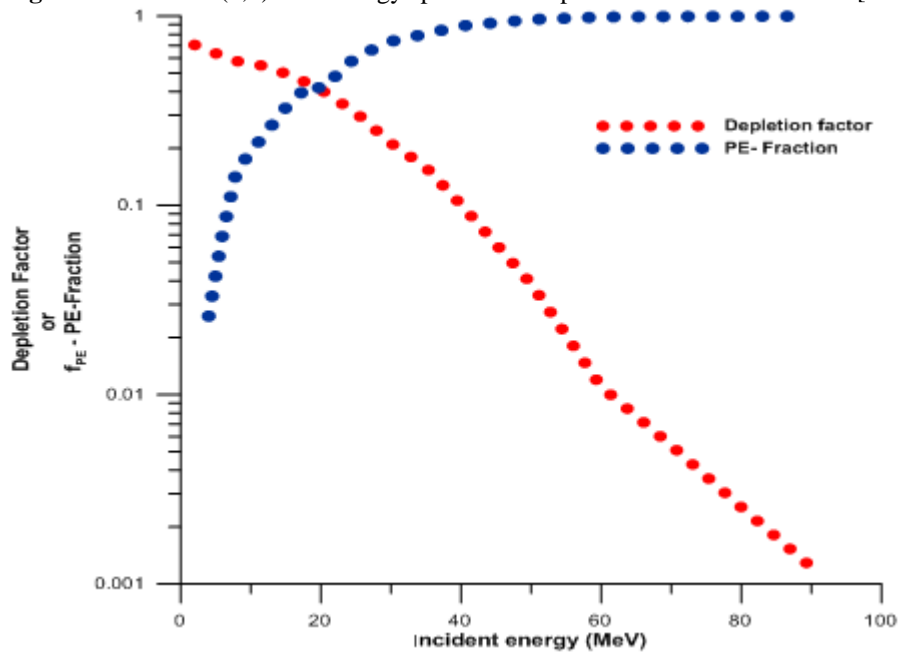


Figure 4: The DF and PE-fraction via incident neutron energy on ^{98}Mo

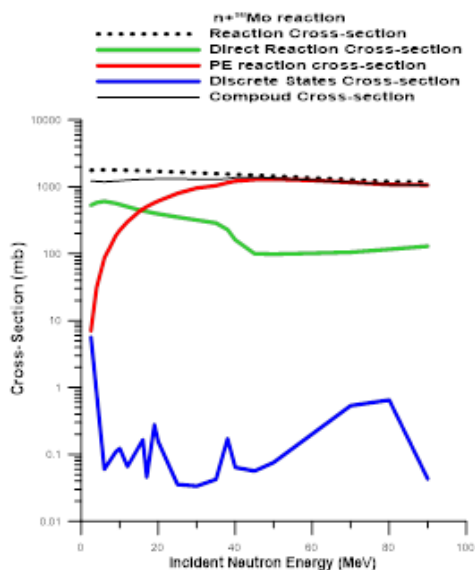


Figure 5: The possible stage's cross-sections in $n+^{98}\text{Mo}$ reaction

References

- [1] J.J. Griffin, Phys. Rev. Lett. 17 (1966) 478.
- [2] F. C. Williams nucl. Phys. A 166(1971) 231.
- [3] V.A. Plyuiko, Yad. Fiz. 27 (1978) 1175.
- [4] J.M. Akkermans, Phys. Lett. B 82 (1979) 20.
- [5] C. Y. Fu Nucl. Sci. Eng. 86 (1984) 344.
- [6] C. Kalbach, Phys. Rev. C 32 (1985) 1157.
- [7] C. Kalbach, Phys. Rev. C 47 (1993) 587.
- [8] J.M. Akkermans, H. Gruppelaar, Phys. Lett. B 157 (1985) 95.
- [9] P. Obložinsk`y, Phys. Rev. C 35 (1987) 407.
- [10] P. Obložinsk`y Nucl. Phys. A453 (1986) 127-140.
- [11] C. Kalbach, Phys. Rev. C 33 (1986) 818.
- [12] C. Kalbach Nucl. Sci. Eng. 95 (1987) 70.
- [13] Y. Alhassid, G. F. Bertsch, S. Liu, and H. Nakada. Phys. Rev. Lett. 84 (2000) 4313.
- [14] S. Hilaire, lecture given in the workshop data and nuclear reactors: Physics, Design and Safety. Trieste, France. 13 March - 14 April 2000. LNS015005.
- [15] C. Kalbach, Z. Phys. A 283 (1977) 401.

- [16] M. Blann, H. Vonach, Phys. Rev. C 28 (1983) 1475.
- [17] M. Blann, Phys. Rev. C 54 (1996) 1341.
- [18] A.J. Koning, M.B. Chadwick, Phys. Rev. C 56 (1997) 970.
- [19] C. A. SoaresPompeia and B. V. Carlson, Phys. Rev. C 74 (2006) 054609.
- [20] C. Kalbch, Phys. Rev. C 73 (2006) 024614.
- [21] C. Kalbach, February 2007, User's Manual for PRECO-2006, Exciton Model Pre-equilibrium Nuclear Reaction Code with Direct Reactions, Triangle Universities Nuclear Laboratory, Duke University.
- [22] W.D. Myers and W. J. Swiatecki, Nucl. Phys. 81 (1966) 1.; M. Herman, G. Reffo and C. Costa. Phys. Rev. C 39 (1989) 1269.
- [23] BROND-2.2, M. N. Nikolaev, G. N. Manturov, W.N. Kostcheev, EVAL-NOV83, J., YK, V.1, P.50 (1983).
- [24] Evaluated nuclear data file (ENDF) database Version of 2017-06-01 (<https://www-nds.iaea.org/exfor/endl.htm>)
- [25] A.V. Voinov, S.M. Grimes, C.R. Brune, M.J. Hornish, T.N. Massey, A. Salas, Phys. Rev. C 76 (2007) 044602.
- [26] C. Kalbach, Acta Phys. Slov. 45 (1995) 685.
- [27] G. S. Mani, M. A. Melkanoff, and I. Iori, Centre d'Etudes Nucléaires de Saclay report CEA 2380 (1963).
- [28] F. D. Becchetti, Jr., and G.W. Greenlees, Phys. Rev. C 182 (1969) 1190.
- [29] Mahdi H. Jasim, Zaheda A. Dakhil and Rasha S. Ahmed, "The transition rates for ^{232}Th using the two-component particle-hole state density with different corrections" Iraqi Journal of Science, 2013, Vol.54, No .1, Pp.115-120.
- [30] H. Feshbach and V. Weisskopf, Phys. Rev. 76 (1949) 1550.]
- [31] M. M. Shapiro, Phys. Rev. 90 (1953) 171.
- [32] I. Dostrovsky, Z. Frankel and G. Friedlander, Phys. Rev. 116 (1959) 683.
- [33] A. Chatterjee, K. H. N. Murthy, and S. K. Gupta, Pramana 16 (1981) 391.
- [34] M. Guttormsen, T. Ramsøy, and J. Rekestad, Nucl. Instrum. Methods Phys. Res. A 255 (1987) 518.
- [35] A. Schiller, L. Bergholt, M. Guttormsen, E. Melby, J. Rekestad, and S. Siem, Nucl. Instrum. Methods Phys. Res. A 447 (2000) 498.
- [36] W. Hauser and H. Feshbach, The Inelastic Scattering of Neutrons, Phys. Rev. 87 (1952) 366.
- [37] P. Demetriou, S. Goriely, Microscopic nuclear level densities for practical applications, Nucl. Phys. A 695 (2001) 95-105.
- [38] T. Von Egidy and Dorel Bucurescu, Systematics of nuclear level density parameters Phys. Rev. C 72 (2005) 044311.
- [39] K. SurendraBabu, Young-Ouk Lee, S. Mukherjee, Analysis of charged particle induced reactions for beam monitor applications, Nucl. Instr. and Meth. in Phys. Res. B, Vol. 283 (2012) 46-54.
- [40] EXFOR Nuclear reaction data, (<http://www-nds.iaea.org/exfor/>), (<http://www.oecdnea.org/janisweb/search/exfor/>) and (<http://www.nndc.nsl.gov> (CSISRS)).